JCAMECH

Vol. XX, No. XX, XX 20XX, pp 307-318
DOI: 10.22059/jcamech.2017.237353.160

Multi-objective Optimization of web profile of railway wheel using Bi-directional Evolutionary Structural Optimization

Ali Asghar Atai[1,*], Ehsan Azarlu[2]

[1] *School of Mechanical Engineering, College of Engineering, University of Tehran, Iran.*

[2] *Mechanical Engineering Department, Islamic Azad University-Karaj Branch, Karaj, Iran*

Received: 9 July. 2017, Accepted: 20 Sep. 2017

Abstract

In this paper, multi-objective optimization of railway wheel web profile using bidirectional evolutionary structural optimization (BESO) algorithm is investigated. Using a finite element software, static analysis of the wheel based on a standard load case, and its modal analysis for finding the fundamental natural frequency is performed. The von Mises stress and critical frequency as the problem objectives are combined using different weight factors in order to find the sensitivity number in the method, which specifies which elements to be omitted and which to be added. The iterative process is continued until convergence to an a priori specified material volume. The resulted web profiles show that when the stress is important, material removal is from the middle part of the web, while for frequency as the important objective, the removal is from near the rim part of the web. The suggested profile, corresponding to equal weight factor for the objectives, has a better volume and stress state compared to a standard web profile, and has a more uniform stress distribution. However, higher natural frequency, compared to that of the standard profile, are obtained for larger frequency weight factors, although with a bigger volume. In the end, considering manufacturability of the wheel, the jagged profile resulted from BESO is replaced with a fitted smooth curve and performing the finite element analysis on it. It is seen that there is an improvement in the obtained objectives for the smoothened profile, with no significant change in volume.

Keywords: BESO, Topology optimization, Railway wheel, Multi-objective optimization**.**

[*] Corresponding Author. Tel.: +98 21 61119951; Fax: +98 21 88013029
Email Address aataee@ut.ac.ir

1. Introduction

Topology optimization is one of interesting and important fields of structural engineering, looking for the best possible placement of material in the structure so that while the loads are carried safely, minimum amount of material is used. For continuous structures, such as 2D and 3D beams, columns, even micro-structures, different methods of topology optimization, such as SIMP (Solid Isotropic Material with Penalization), ESO (Evolutionary Structural Optimization), and BESO (Bidirectional Evolutionary Structural Optimization) are developed. These methods start with an initial material domain and gradually, add and/or delete material to/from regions which has great/little positive effect on structural performance, which might be measured by stiffness, strain energy, stress distribution, etc. Since early development of ESO by Xie and Steven [1], it was employed for optimizing structural performance, such as buckling [2]. In ESO, only material elimination was performed, starting from a sufficiently large continuum, and gradual inefficient material removal. It was then changed to AESO (Adaptive Evolutionary Structural Optimization), in which material addition in high gradient places was performed. BESO, combined the advantages of both, considering simultaneous addition/elimination of material. Huang and Xie improved the performance of BESO by eliminating mesh dependency and facilitating convergence [3], and applied it to several structural problems, and from there several authors used the method for various static and dynamic optimization of structures, including solid-fluid interaction applications [4-5]. In order to present an overall comparison of the methods stated above, ESO has the shortcoming just material elimination, and thus the initial continuum must be large enough to encounter the expected final optimum configuration. Moreover, once a material is eliminated during the iterative process of this method, it is not possible to bring it back if it would be needed for the optimum topology. SIMP is quite similar to BESO, except that it considers a continuous variable for material existence, which starts at an initial value and is gradually moving towards 1 (presence of material) or zero (elimination of material), resulting in the final topology. The first author's experience with the method has shown that the success and convergence of the method is much dependent on how the material existence parameter is updated in each iteration, and it may diverge. While BESO suffers much less from this problem, by considering a binary material existence variable. There are researchers that support either method, but BESO has gained a popularity of its own and some believe that "BESO has great potential, especially considering the latest enhancements, especially when combined with other techniques like genetic algorithms" [6].

In terms of the application considered in this work, a railway wagon wheel is considered here. Wheels function both as carrying wagon load (statically and dynamically), and conducting the wagon in its railway. There are different types of wheels based on the type of wagon and loading on them, some of which are shown in Fig. 1 [7]. There are also profiles claimed to be of lesser stress under loading, and of standard profiles in different parts of the world [8] (see Fig. 2).

There are few researches regarding the optimization of performance of wagon wheels. Hirakawa and Sakamoto studied the variation of effective parameters on fracture of wheels [9]. Nielsen and Fredö used the method design of experiments for optimization of wheels. This justifies our motivation for a new research in this field, especially for applying BESO to a 3D round structure, for multi-objective optimization.

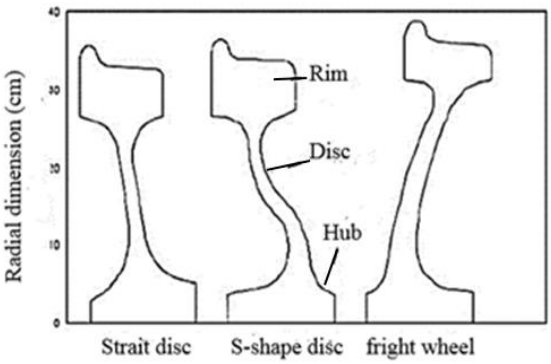

Fig. 1 Different types of wheel web profiles [6]

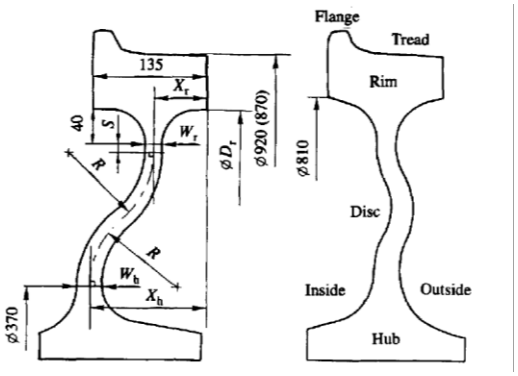

Fig. 2 (a) Low-stress wheel, (b) EN standard wheel [7]

In this work, multi-objective optimization of the wagon wheel, considering uniformity of stress distribution and natural frequency of the wheel is studied. In the next section, the method of BESO, tailor-made for multi-objective optimization of the problem at hand is explained in detail. In section 3, finite element modeling and static and dynamic analysis of the wheel, needed to extract BESO parameters are explained, and resulted

optimized wheel web profiles, considering different weight factors (priorities) for the objective are presented. The recommended compromise profile is further analyzed, by smoothening the jagged web profile resulted from FE-BESO, in order to take manufacturability into account. It is shown that the modified optimized profile considerably outperforms the standard wheel profile, at least in the frame of the two objectives considered.

2. Method of BESO for multi-objective optimization

In This section, the method of BESO, which is modified to be suited for the current multi-objective optimization problem at hand, is explained in detail.

BESO is an evolutionary structural optimization method with the property of both eliminating the less efficient material elements from the structure, and adding a previously eliminated material element, which now proves to be efficient, in each iteration of an iterative procedure. Decision on eliminating or adding elements is based on an element-wise parameter, called sensitivity number, which shows the sensitivity of the objective(s) to the design variable (here, presence or absence of elements). Formally, BESO tries to minimize a characteristic property of structure volume constraint for the structure, as follows

$$\begin{aligned} &Minimize\ f = \sum_{i=1}^{N} P_i \\ &Subject\ to\text{:}\quad V^* - \sum_{i=1}^{N} V_i x_i = 0 \\ &x_i = 0 \text{ or } 1 \end{aligned} \qquad (1)$$

in which f is the objective function, N is the number of elements, $\boldsymbol{P_i}$ is some characteristic property of the ith element (such as stiffness, von-Mises stress, contribution to natural frequency, etc.), V_i is the volume of the ith element, V^* is the target volume for the structure, and x_i shows the existence (1) or absence (0) of the ith element.

But instead of direct minimization of objective, its sensitivity to the existence/absence of elements is taken into account, which causes some live elements to die, and some dead elements to become live, subject to a gradual evolution of the volume of the structure that approaches the target volume V* upon convergence.

In this work, the wheel is considered both from static and from dynamic point of view. Usually for static performance in BESO, the stiffness or strain energy of the structure is the objective. But there are alternatives minimizing the average von-Mises stress in the structure [10]. It can be shown that these two schemes are almost equivalent [11]. In the work, the second scheme is adopted because the von-Mises stress is readily available from finite element analysis. In this regard, the sensitivity parameter of this objective for the ith element is taken as

$$\alpha^e_{i,static} = \sigma^e_{Vonmises} \qquad (2)$$

in which, $\boldsymbol{\sigma^e_{Vonmises}}$ is the von-Mises stress for the ith element. As for the dynamic (natural frequency) analysis, the sensitivity parameter is taken to be [12]

$$\alpha^e_{i,dynamic} = \frac{1}{m_i}\{\emptyset^e_i\}^T(\omega_i^2[M^e] - [K^e])\{\emptyset^e_i\} \qquad (3)$$

in which $\boldsymbol{m_i}$, $\{\emptyset^e_1\}$, $[\boldsymbol{M^e}]$, and $[\boldsymbol{K^e}]$ are the mass, element displacement vector based on the first mode shape, mass matrix and stiffness matrix of the ith element, respectively, and $\boldsymbol{\omega_1}$ is the first natural frequency.

Topological optimization looks for a more uniformly stressed structure with the least amount of material. Therefore, the optimization problem is stated in its simplest form as follows with a volume constraint**.**

Before combining the sensitivity numbers to a single one for a combination of objectives, they are normalized in the interval [0, 1] as follows in order to make the combination meaningful

$$\alpha^{\mathrm{e}}_{\mathrm{i,NS}} = \frac{\alpha^{\mathrm{e}}_{\mathrm{i,static}} - \alpha^{\mathrm{max}}_{\mathrm{static}}}{\alpha^{\mathrm{max}}_{\mathrm{static}} - \alpha^{\mathrm{min}}_{\mathrm{static}}} \qquad (4)$$

$$\alpha^{\mathrm{e}}_{\mathrm{i,ND}} = \frac{\alpha^{\mathrm{e}}_{\mathrm{i,dynamic}} - \alpha^{\mathrm{max}}_{\mathrm{dynamic}}}{\alpha^{\mathrm{max}}_{\mathrm{dynamic}} - \alpha^{\mathrm{min}}_{\mathrm{dynamic}}} \qquad (5)$$

in which $\alpha^e_{i,NS}$ and $\alpha^e_{i,ND}$ are the normalized sensitivity number for static and dynamic analysis, respectively, and the superscripts min and max indicate the minimum and maximum corresponding sensitivity numbers among all elements, respectively.

Next, analogous to the combination of multi-objectives into a single one using the weighted sum, the multi-objective sensitivity number for each element of the structure is defined by

$$\alpha^e_{i,multi} = \lambda_s(\alpha^e_{i,NS}) + \lambda_m\ (\alpha^e_{i,ND}) \qquad (6)$$

in which λ_s and λ_m are the weight factors for the static and dynamic objectives, respectively, varying in the range [0, 1], showing the importance of each objective. In the numerical part, these weight factors are related by $\lambda_s = \lambda_m - 1$, and are varied in the range to get topologies with different priority for the objectives, as it will be seen in the next section.

One of the main issues in ESO is that since the structure is discretized into elements, the sensitivity numbers, which determine which elements are eliminated or added, become discontinuous and therefore result a checkerboard pattern (see Fig. 3) in the optimized structure, which is unacceptable from manufacturability point of view. To overcome this problem in BESO, the element sensitivity numbers are redefined as follows in order to smoothen their distribution. This also helps the

method to become mesh-independent (different mesh sizes give rise to more or less the same optimized structure) [10].

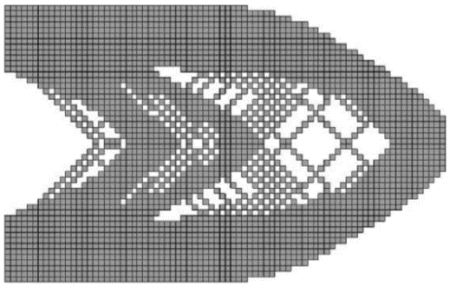

Fig. 3 An example of checkerboard pattern in the ESO method [10]

The technique, which is called filtration, goes as follows. First, for every node *j* in the domain, the nodal sensitivity number is calculated by

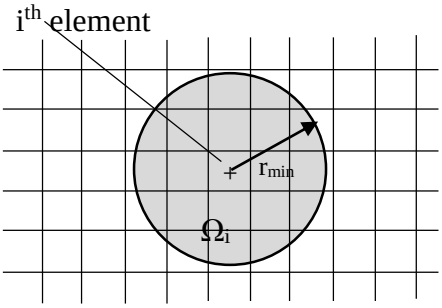

Fig. 4 Circular subdomain of the ith element for smoothening the sensitivity numbers

$$\alpha_j^n = \sum_{i=1}^{M} w_i \alpha_i^e \tag{7}$$

in which M is the total number of elements common at node j, and w_i is the weight factor of the ith element given by

$$w_i = \frac{1}{M-1}\left(1 - \frac{r_{ij}}{\sum_{i=1}^{M} r_{ij}}\right) \tag{8}$$

with the property

$$\sum_{i=1}^{M} w_i = 1 \tag{9}$$

Here, r_{ij} is the distance from the center of ith element to node *j*. The above definition of weight factors implies that element sensitivity number has greater effect on closer nodes. Next, these nodal sensitivity numbers are used to smoothen the element sensitivity number throughout the mesh. For every element *i*, a circular subdomain Ω_i with its center at the center of the element and with a radius of r_{min} is considered (Fig. 4). The parameter r_{min} plays the role of identifying nodes that influence the sensitivity of ith element. It should be large enough so that at least one element surrounding the ith element is included in the domain. On the other hand, in this scheme, the size of the subdomain is kept constant, irrelevant of the mesh size. Having the sensitivity numbers of all nodes in the domain, the sensitivity number of ith element is redefined as

$$\alpha_i^e = \frac{\sum_{j=1}^{k} w(r_{ij})\alpha_j^n}{\sum_{j=1}^{k} w(r_{ij})} \tag{10}$$

in which k is the total number of nodes in the subdomain and $w(r_{ij})$ is the linear weight factor defined by

$$w(r_{ij}) = r_{min} - r_{ij} \qquad (j = 1,2,\dots,k) \tag{11}$$

This filtration scheme helps to eliminate both checkerboard pattern and mesh dependency. Another problem is the instability in the process, which may show oscillations in the evolving topology during the process. To remedy this issue, the history of evolutions of sensitivity numbers is taken into account by defining

$$\alpha_i^k = \frac{\alpha_i^k + \alpha_i^{k-1}}{2} \tag{12}$$

in which k is the current iteration number and the updated sensitivity number is used for the next iteration.

In order to reach the target volume V^* upon convergence, in the iterative process, a target volume V_{k+1} is considered for the next iteration, which is changed step by step until the final target volume V^* is reached. It is this iterative target volume which governs how many elements should be added to or deleted from the current topology. This volume is defined by

$$V_{k+1} = V_k(1 \pm ER) \qquad (k = 1,2,3,\dots) \tag{13}$$

in which ER is the evolutionary volume ratio (The plus/minus sign is for the case where the starting volume is less/greater than the final target volume). This parameter should be set at a reasonable value so that there is a smooth gradual change of topology from each iteration to next. Once the target volume V^* is reached in an iteration, it is kept constant for the remaining iterations, i.e. $V_{k+1} = V^*$.

To decide which elements to be added or deleted in each iteration, the sensitivity number of each element for the whole domain is calculated as explained above, and sensitivity numbers are sorted (it should be noted that void elements also get a nonzero sensitivity number based on the filtration scheme). Threshold sensitivity numbers α_{del}^{th} and α_{del}^{th} are considered for deleting and adding elements respectively. For the ith element, if $\alpha_i \leq \alpha_{del}^{th}$, then that element is deleted (x_i is set to 0), and if $\alpha_i \geq \alpha_{add}^{th}$, the element is added ($x_i$ is set to 1). The thresholds are set in each iteration so that the target volume V_{k+1} for the next iteration is met. Furthermore, a parameter AR_{max} (maximum volume addition ration, i.e. maximum of the ratio of added elements to the total number of elements in the domain) controls how many elements are added in each iteration, in order to avoid loss of integrity of topology in case to many elements are to be added.

As a convergence criterion, both the target volume and the combined objective function corresponding to the combined sensitivity number (i.e. $\lambda_s \times$ maximum von-Mises stress + $\lambda_m \times$ negative of the first natural frequency) are tracked and if their change is less than a certain tolerance, then the procedure stops.

3. In summary, the flowchart for the multi-objective BESO is presented in Fig. 5.

4. Modeling , analysis, and optimization

Finite element analysis lies at the core of BESO. Therefore, the usual sequence of introducing geometry, material, meshing, loading and boundary conditions, and analysis used in commercial FE software is explained here.

Fig. 6 shows the cross section of a so-called "s-shaped" wheel. It is used in this research for its rim, hub, and overall dimensions. These dimensions are taken from standard no. UIC 515-1 [13]. In order to have a more realistic wheel-rail interaction during loading, the rim is modeled using the detailed geometry from this standard, shown in Fig. 7. The geometry of the web is what we try to optimize using BESO. But the geometry shown in Fig. 6 is used later on for comparison with the optimized wheel.

For rail modeling, the geometry is taken from standard UIC-60, shown in Fig. 8 [15].

Next, the material is defined, which is steel in this case with properties E=200 GPa, $\vartheta = 0.3$, and ρ=7800 kg/m^3.

In the meshing part, a 3D model of the wheel is generated. First, the cross section of the wheel with a block for the web (which will be emptied later on using BESO) is considered (Fig. 9) as an area and is meshed. Next, the meshed area is revolved about the wheel axis to generate the 3D wheel, with 20 sectors and 8 divisions in each sector, made of SOLID185 elements (Fig. 10). To get the proper mesh size, a mesh sensitivity analysis was done with a typical run. The wheel cross section was divide using different mesh sizes and the maximum von-Mises stress obtained was taken as the converge parameter. The hardware was an Intel(R) Corei5 system with 8GB of RAM. The results are shown in table 1. For the finest mesh size in the table, the hardware was not able to give a result. Based on the von-Mises stress values and hardware limitations, a mesh size of 5 by 5 was considered as appropriate for all the analyses.

For boundary conditions, since the wheel hub is connected to the axle almost rigidly, all the displacements and rotations for the inner surface of the wheel hole were set to zero.

As for the loading, the BS EN_13979 standard considers different load cases with point loads on the wheel rim [16]. One of these cases is for the wheel moving in straight line (Fig. 11). In this case, a vertical load of F_z with a magnitude of 1.25 times the wagon weight per wheel must be applied at the point indicated. In order to have a better grasp of wheel-rail interaction for this loading, part of the rail was modeled and meshed and was brought into contact with the wheel at the point of F_z. The external loads on the rail were set in an equivalent manner so that the standard load Fz would be on the wheel (Fig. 12). For the case study considered here, a force of F_z=98.8 kN was applied on the wheel.

Once the model is prepared, two types of analyses are done as follows in order to calculate the sensitivity numbers for BESO:

1- A static analysis is performed with the defined loading to get the von-Mises stress as the static sensitivity number (Eq. 4).

2- To get the frequency sensitivity number, a modal analysis is done and based on the mass and stiffness matrices of elements, and the first natural frequency, the sensitivity number is calculated using Eq. (5).

These two analyses are performed using a macro for the FE software in each iteration of BESO.

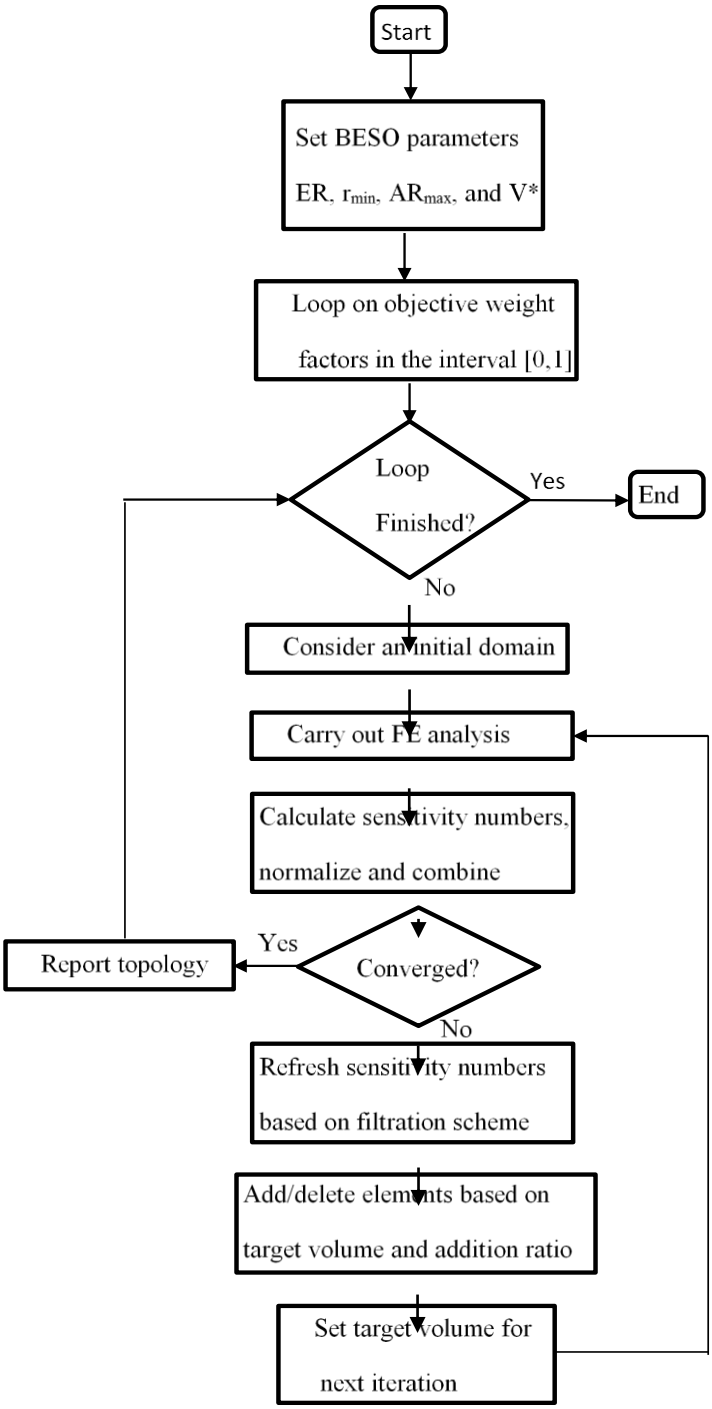

Fig. 5 Flowchart of multi-objective BESO

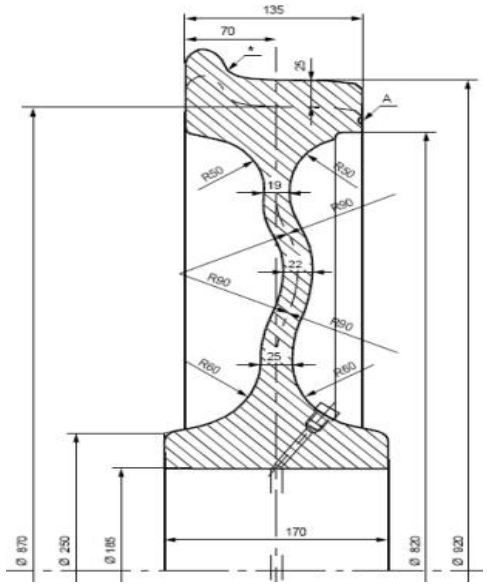

Fig. 6 Cross-section of EN standard wheel [14] (dimensions in mm)

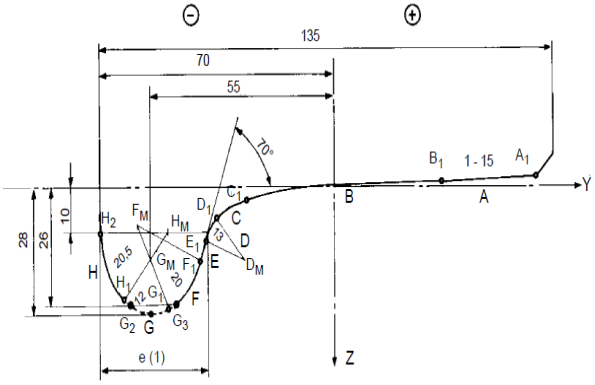

Fig. 7 Geometry of standard wheel rim with 100-720 mm diameter [13]

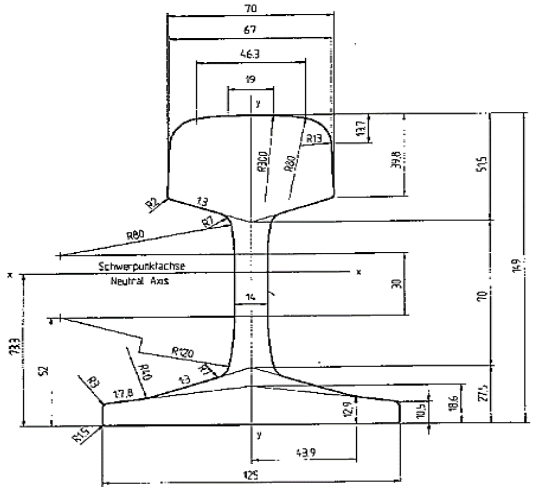

Fig. 8 Geometry of UIC-60 rail [15] (dimensions in mm)

Table 1. Mesh sensitivity analysis

Mesh size	Total number of nodes	Total number of elements	Maximum von-Mises stress (Pa)
10mm×10mm	83858	73452	0.779×10^{9}
7.5mm×7.5mm	123538	111852	0.861×10^{9}
5mm×5mm	230578	215852	0.884×10^{9}
2.5mm×2.5mm	782526	758384	NA

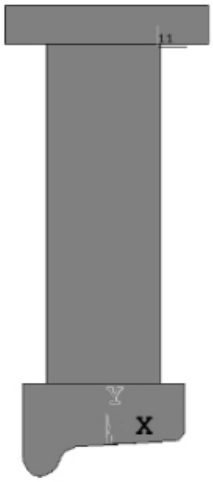

Fig. 9 Creation of wheel cross section

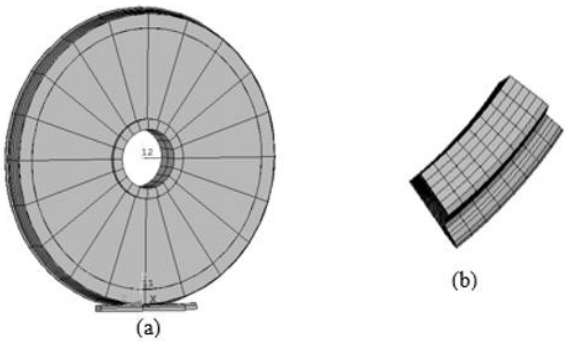

Fig. 10 (a) A wheel with 20 sectors, (b) 3D meshing of sectors

Experimenting with the method, the following BESO parameters proved to be promising for the problem at hand:

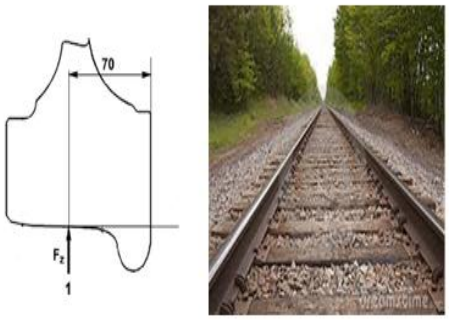

Fig. 11 Straight path and loading point on the wheel for this case [16]

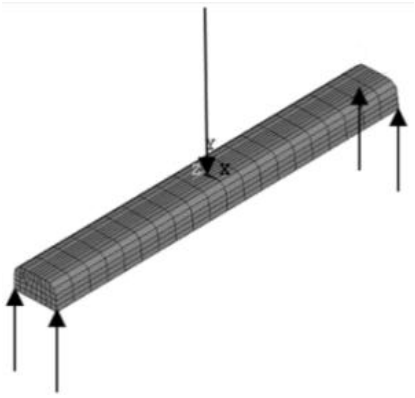

Fig. 12 Equivalent rail loading for standard force on the wheel

$V^* = 0.1\mathrm{V}_{total}$, r_{min} =12.5mm, AR_{max} =0.5, ER = 0.03

The multi-objective optimization was performed using weighted sum method and considering weight factors λ_s and λ_m, for static and dynamic analysis sensitivity numbers, respectively.

Fig. 13 shows the resulted web profile based on different weight factor combinations. It is seen that when the dynamic response is less important (lower values of λ_m), the web is thinner in the middle, but once the critical frequency becomes of greater importance (higher values of λ_m), the web becomes thinner at the rim junction. This could be justified by considering the web like a beam. When lower maximum stresses are needed, the beam becomes thicker at both ends, which are closer to loads, to diminish the stress. On the other hand, when high natural frequencies are needed, the beam becomes thicker close to the rigid end (hub) to increase the stiffness and thus the frequency. Another interesting point is that when static response becomes important ($\lambda_s = 1$), the stress tends to be more uniform throughout the web, which is a good sign that BESO is working.

Figs. 14 to 16 are a proof of convergence of BESO, for different weight factors. They show that both the volume fraction and von-Mises stress reach asymptotically to a final value as the iteration number is increases. They are comparable to Fig. 3.3 of Ref. 17.

In order to make a comparison between the optimized wheel and the standard one, an FE model of the standard wheel is generated and evaluated statically and dynamically (Fig. 17). It is seen that the stress distribution in the standard wheel is less uniform compared to that of the optimized wheel ($\lambda_s = 1$) in Fig. 15. The performance of the standard wheel and those of BESO with different weight factors are presented in table 2. It is seen that all the BESO wheels have a somewhat lesser volume than that of the standard wheel. The BESO wheels have lower maximum von-Mises stresses (for higher values of λ_s) and higher natural frequencies (for lower values of λ_s), than those of the standard wheel, which is expected.

To introduce a compromise optimum solution, the profile of ($\lambda_s = 0.5\,, \lambda_m = 0.5$) , is suggested, with a volume of about 3 percent less than that of the standard wheel, a lower maximum von-Mises stress, and a comparable natural frequency.

In order to address the manufacturability of the optimized wheels, the suggested compromise web profile with jagged edges is considered and the edges are smoothened with a polynomial curve (Fig. 18). The modified, smoothened profile is re-analyzed to see how the performance is changed. Fig. 19 shows the von-Mises stress distribution for this profile, and the performance values are given in table 3. It is seen that the volume increase is negligible compared to the original BESO profile. But more importantly, the maximum von-Mises stress is decreased 17.5 percent, and the natural frequency is increased by 11.5 percent, compared to the standard wheel. This shows the ability of BESO in making lighter structures with high performance.

5. Conclusion.

In this work, multi-objective optimization of railway wheel web profile was investigated using BESO. Static and dynamic performance of the wheel where analyzed using finite element. Based on the combined sensitivity number and with different static and dynamic objective weight factors, different web profiles were obtained, with a better static and/or dynamic performance compared to the standard wheel. The compromise suggested solution with smoothened profile edges outperformed the standard one significantly. As a final note, it should be stated that due to lack of enough information and equipment, it was not possible for the authors to do a verification of the findings. It is suggested as a future work to do experiments on the suggested optimal wheel, to verify that indeed is optimum or close to it.

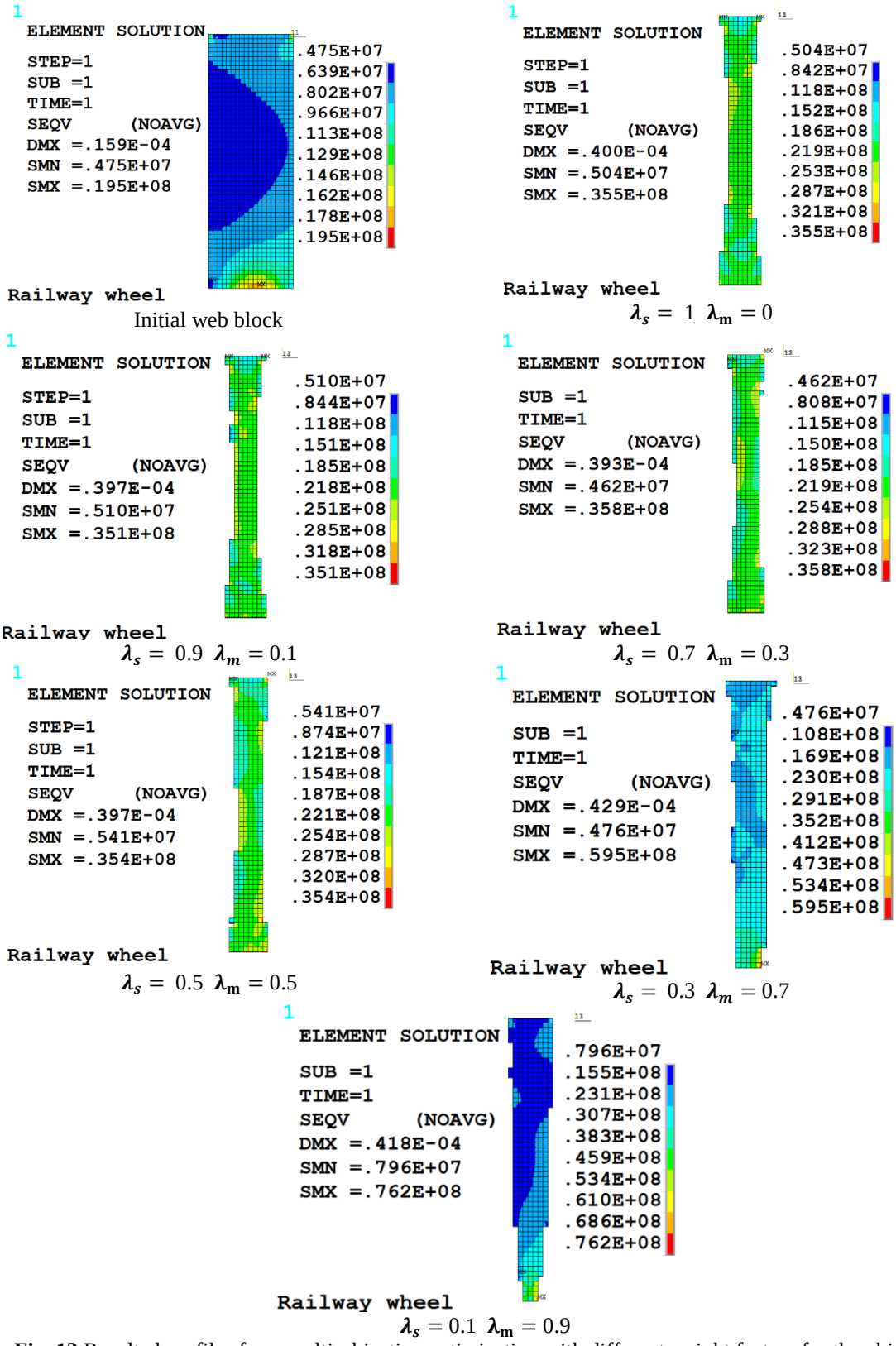

Fig. 13 Resulted profiles from multi-objective optimization with different weight factors for the objectives

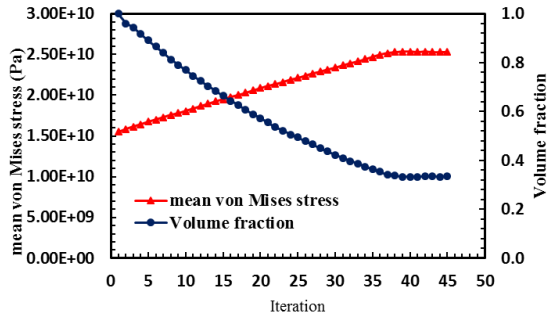

Fig. 14 History of mean von Mises stress and volume fraction for $\lambda_m = 0$, $\lambda_s = 1$

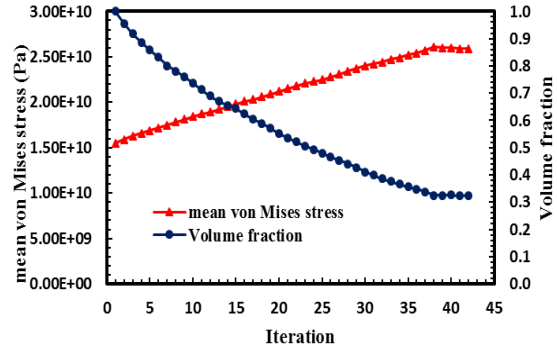

Fig. 15 History of mean von Mises stress and volume fraction for $\lambda_m = 0.5$, $\lambda_s = 0.5$

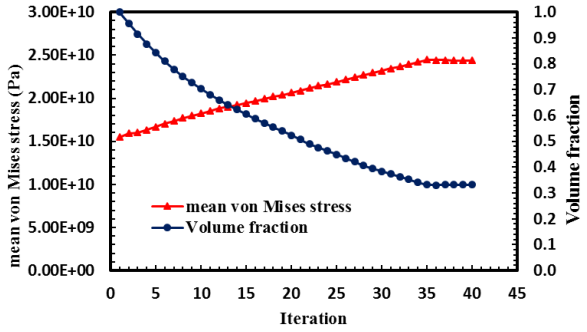

Fig. 16 History of mean von Mises stress and volume fraction for $\lambda_m = 0.9$, $\lambda_s = 0.1$

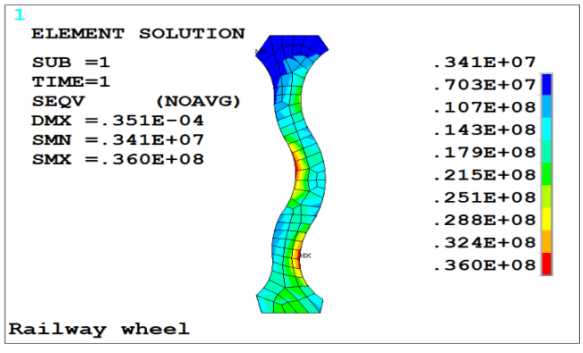

Fig. 17 von Mises stress distribution for EN standard wheel

Table 2. Comparison of volume, maximum von-Mises stress and first natural frequency of standard and optimized wheel web profile

wheel web profile (Figs. 8 & 15)	volume (10^{-3} m^3)	Maximum von-Mises stress (10^8 Pa)	First natural frequency (HZ)
Standard	0.1902	0.360	**118.6695**
$\lambda_m = 0$ $\lambda_s = 1$	0.1899	0.355	**101.4532**
$\lambda_m =$ **0.1** $\lambda_s =$ **0.9**	0.1895	0.351	**103.0177**
$\lambda_m =$ **0.3** $\lambda_s =$ **0.7**	0.1875	0.357	**102.60**
$\lambda_m =$ **0.5** $\lambda_s =$ **0.5**	0.1850	0.354	**105.0534**
$\lambda_m =$ **0.7** $\lambda_s =$ **0.3**	0.1890	0.597	**121.834**
$\lambda_m =$ **0.9** $\lambda_s =$ **0.1**	0.1887	0.764	**124.1121**

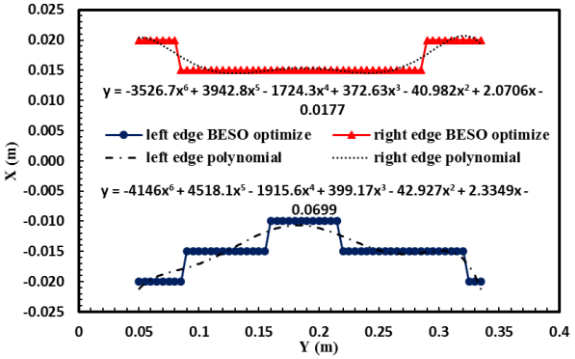

Fig. 18 Smoothening of the discontinuous optimized profile, $\lambda_m = 0.5$, $\lambda_s = 0.5$

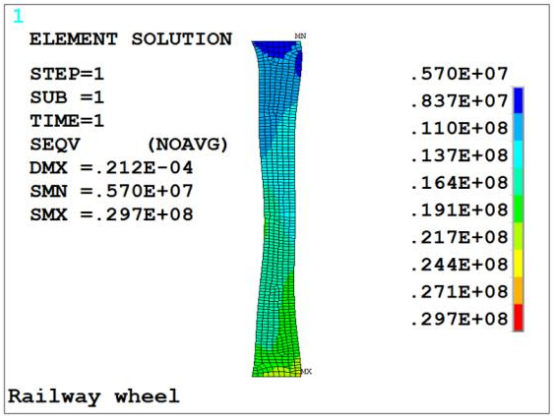

Fig. 19 Distribution von Mises stress for smoothened profile.

Table 3. Volume, maximum von Mises stress and first natural frequency for the optimized smoothened profile

Volume $10^{-3}(m^3)$	**Maximum von-Mises stress** 10^8 (Pa)	**Natural frequency** (HZ)
0.18757	0.297	132.367

References

[1] Xie, Y.M. and G.P. Steven, A simple evolutionary procedure for structural optimization. Computers & structures, 1993. 49(5): p. 885-896.

[2] Manickarajah, D., Y. Xie, and G. Steven, Optimisation of columns and frames against buckling. Computers & Structures, 2000. 75(1): p. 45-54.

[3] Huang, X. and Y. Xie, Convergent and mesh-independent solutions for the bi-directional evolutionary structural optimization method. Finite Elements in Analysis and Design, 2007. 43(14): p. 1039-1049.

[4] Shabani Nodehi .S, S. R. Falahatgar, R. Ansari, Studying the effects of design parameters on the final topology of planar structures by improved bi-directional evolutionary Structural optimization method, Modares Mechanical Engineering, Vol. 16, No. 5, pp. 29-38, 2016. (in Persian)

[5] Shobeiri, V., The topology optimization design for cracked structures. Engineering Analysis with Boundary Elements, 2015. 58: p. 26-38.

[6] Cazacu R, Grama L. Overview of structural topology optimization methods for plane and solid structures. Annals of the University of Oradea, Fascicle of Management and Technological Engineering. 2014 Dec.

[7] Farzanegan.M,A.Ohadi Esfehani, S. H. Hoseini, Investigating the effect of web curvature of wagon wheel on itsphysical performance using, FEM,15th annual international ISME conference, 2007. (in Persian)

[8] Fermér, M., Optimization of a railway freight car wheel by use of a fractional factorial design method. Proceedings of the Institution of Mechanical Engineers, Part F: Journal of Rail and Rapid Transit, 1994. 208(2): p. 97-107.

[9] Hirakawa, K. and H. Sakamoto, Effect of design variation on railroad wheel fracture. ASME paper, 1981.

[10] Huang, X. and M. Xie, Evolutionary topology optimization of continuum structures: methods and applications. 2010: John Wiley & Sons.

[11] Liang, Q.Q., Y.M. Xie, and G.P. Steven, Optimal topology selection of continuum structures with displacement constraints. Computers & Structures, 2000. 77(6): p. 635-644.

[12] Cho, K.-H., J.Y. Park, S.P. Ryu, S.Y. Han., Reliability-based topology optimization based on bidirectional evolutionary structural optimization using multi-objective sensitivity numbers. International Journal of Automotive Technology, 2011. 12(6): p. 849-856.

[13] Code, U., 510-2, 2004. Trailing stock: wheels and wheelsets. Conditions concerning the use of wheels of various diameters.

[14] U. Code, 515-1, 2003, Passenger rolling stock – Trailer bogies –Running gear – General provisions applicable to the components of trailers bogies.
[15] U. Code, 861-3 Leaflet 1991, International Union of Railways, 3rd ed.
[16] EN, B., 13979-1. Railway Application-Wheelsets and Bogies-Monobloc Wheels-Technical Approval ProcedurePart1: Forged and Rolled Wheels, 2003.